Atomistic spin model based on a spin-cluster expansion technique: Application to the IrMn₃/Co interface

L. Szunyogh,[1,*] L. Udvardi,[1] J. Jackson,[2,3] U. Nowak,[2] and R. Chantrell[3]

[1]*Department of Theoretical Physics, Budapest University of Technology and Economics, Budafokiút 8. H1111 Budapest, Hungary*
[2]*Fachbereich Physik, Universität Konstanz, D-78457 Konstanz, Germany*
[3]*Department of Physics, University of York, York YO10 5DD, United Kingdom*

In order to derive tensorial exchange interactions and local magnetic anisotropies in itinerant magnetic systems, an approach combining the spin-cluster expansion with the relativistic disordered local moment scheme is introduced. The theoretical background and computational aspects of the method are described in detail. The exchange interactions and site-resolved anisotropy contributions for the IrMn₃/Co(111) interface, a prototype for an exchange bias system, are calculated including a large number of magnetic sites from both the antiferromagnet and ferromagnet. Our calculations reveal that the coupling between the two subsystems is fairly limited to the vicinity of the interface. The magnetic anisotropy of the interface system is discussed, including effects of the Dzyaloshinskii-Moriya interactions that appear due to symmetry breaking at the interface.

I. INTRODUCTION

Spin models form an important tool in the understanding of magnetic systems, particularly of multilayer systems, such as bilayers consisting of ferromagnetic and antiferromagnetic materials, because such models allow the investigation of magnetic configurations and dynamics at the atomic scale. Bilayers of ferromagnetic and antiferromagnetic materials are important parts of the magnetoresistive sensors used, e.g., in hard disk read heads. The role of the antiferromagnetic component is to pin the ferromagnetic layer by the so-called exchange bias effect,[1,2] leading to a shift of the hysteresis loop of the ferromagnet. A number of calculations based on spin models have revealed that the anisotropy of the antiferromagnet and the strength of the interface coupling between the antiferromagnet and the ferromagnet are crucial for the strength and stability of the exchange bias,[3–6] and therefore for the functioning of the device.

IrMn is the most common antiferromagnet industrially because of the large exchange bias and thermal stability that can be obtained with this material. Despite the successful application of this material in exchange bias bilayers, there is still no complete microscopic understanding of the most important parameters, the antiferromagnetic anisotropy and the interface coupling. These properties have recently been inferred by a careful examination of the temperature behavior of the exchange bias of polygranular thin-film bilayers.[7] In order to evaluate the antiferromagnet anisotropy, the magnitude of the exchange bias is fitted to a simple model that depends only upon the grain-size distribution, yielding effective anisotropy and coupling parameters. The origin of the effective anisotropy and interface coupling, due to the microscopic physical properties of the interface, remains, however, inaccessible to direct experimental study.

On the theoretical side, only few first-principles calculations on relativistic effects in Mn-based antiferromagnets have been performed. Regarding the anisotropy, Umetsu *et al.*[8] calculated the magnetic anisotropy energy (MAE) of $L1_0$-type MnTM (TM = Ni, Pd, Pt, Rh, and Ir) compounds and revealed that MnIr had the highest MAE with a value of −7.05 meV/unit cell. Furthermore, a giant second-order

magnetic anisotropy for $L1_2$ IrMn₃ was reported, leading to energy barriers of the order of $K_{eff} = 10.4$ meV/unit cell for rotation of the $T1$ ground-state spin structure around the (111) axis.[9]

The organization of the paper is as follows: in the first part we introduce the concept of the spin-cluster expansion (SCE) merged with the relativistic disordered local moment (RDLM) scheme and discuss the details of the first-principles calculations. Then we present our results for the magnetic moments, the exchange coupling, and the magnetic anisotropy in $L1_2$ IrMn₃, fcc Co bulk, and for the IrMn₃/Co(111) interface. Special attention is paid to the effect of Dzyaloshinskii-Moriya interactions at the interface.

II. THEORY

A. Spin-cluster expansion

Mapping of the energy of an itinerant magnetic system onto a spin Hamiltonian presents a long-standing problem in computational solid-state physics. The most widely used approach relies on an adiabatic decoupling of the longitudinal and transverse spin fluctuations, determined by the fast motion of mobile electrons, $\tau_e \simeq 10^{-15}$ s, and the slow motion of spins, $\tau_{sf} \simeq 10^{-13}$ s. Under such circumstances, time-dependent density functional theory can be approximated by a Landau-Lifshitz equation of motion for the classical spin variables, i.e., the orientation field $\vec{e}(\vec{r},t)$, as combined with spin-density functional theory (SDFT) within the local spin-density approximation (LSDA).[10] Further simplification of the theory is represented by the rigid spin approximation, in which the orientation of the spins is allowed to change from atomic cell to atomic cell. A system of N spin moments is thus characterized by the set of orientations (spin configurations) $\{\vec{e}\} = \{\vec{e}_1, \ldots, \vec{e}_N\}$, with $|\vec{e}_i| = 1$. The energy (grand potential) of the system, $\Omega(\{\vec{e}\})$, determined within LSDA, then defines a classical Hamiltonian that can be used in spin-dynamics simulations.

In order to ensure that the process is tractable, a suitable parametrization must be applied to $\Omega(\{\vec{e}\})$. The simplest reliable approximation, an (extended) Heisenberg model, is

of second order:

$$\Omega(\{\vec{e}\}) = \Omega_0 + \sum_{i=1}^{N} \vec{e}_i \mathbf{K}_i \vec{e}_i + \frac{1}{2} \sum_{\substack{i,j=1 \\ (i \neq j)}}^{N} \vec{e}_i \mathbf{J}_{ij} \vec{e}_j , \qquad (1)$$

where $\mathbf{K}_i$ and $\mathbf{J}_{ij}$ are the second-order anisotropy matrices (which are traceless and symmetric) and the tensorial exchange interactions, respectively. The relativistic torque method (RTM), which was introduced in Refs. 11 and 12, allows the evaluation of these parameters using relativistic electronic structure calculations. By using the RTM, one is required to choose a reference magnetic configuration; usually the ferromagnetic state is taken. For complex magnetic structures, however, the use of such a reference state might lead to incorrect results concerning, e.g., the magnetic ground state of the system.[13] Another drawback of the RTM is that for systems with reduced point-group symmetry the derivation of the anisotropy matrix $\mathbf{K}_i$ might be quite a cumbersome task. More importantly, the RTM is not directly applicable to the calculation of more complicated two-spin interactions, such as biquadratic coupling or multispin interactions, known to be present in magnetic systems at the nanoscale.[13,14]

The spin-cluster expansion (SCE) developed by Drautz and Fähnle[15,16] in principle solves the problems mentioned previously, in that it provides a systematic parametrization of the adiabatic magnetic energy of general classical spin systems. In the following we briefly outline the method. Considering clusters of n sites ($0 \leqslant n \leqslant N$), $C_n \subset I_N = \{1,2,\ldots,N\}$, the functions

$$\Phi_{C_n}^{L_{i_1},\ldots,L_{i_n}}(\{\vec{e}\}) = \frac{1}{(4\pi)^{(N-n)/2}} \prod_{i_k \in C_n} Y_{L_{i_k}}(\vec{e}_{i_k}),$$
$$L_{i_k} = (\ell_{i_k}, m_{i_k}) \neq (0,0) \qquad (2)$$

form an orthonormal and complete basis set of the function space over $\{\vec{e}\}$. Here $Y_L(\vec{e})$ denotes, for convenience, real spherical harmonics. The grand potential of the system can, therefore, be readily expanded as

$$\Omega(\{\vec{e}\}) = \sum_{C_n} \sum_{L_{i_1},\ldots,L_{i_n} \neq (0,0)} J_{C_n}^{L_{i_1},\ldots,L_{i_n}} \prod_{i_k \in C_n} Y_{L_{i_k}}(\vec{e}_{i_k}), \quad (3)$$

where the multispin interactions $J_{C_n}^{L_{i_1},\ldots,L_{i_n}}$ are defined as

$$J_{C_n}^{L_{i_1},\ldots,L_{i_n}} = \int d^2 e_{i_1},\ldots,d^2 e_{i_n} \langle \Omega \rangle_{\vec{e}_{i_1},\ldots,\vec{e}_{i_n}} \prod_{i_k \in C_n} Y_{L_{i_k}}(\vec{e}_{i_k}).$$
$$(4)$$

In the above equation, the key quantities of the theory, namely, the restricted averages of the grand potential are

$$\langle \Omega \rangle_{\vec{e}_{i_1},\ldots,\vec{e}_{i_n}} = \frac{1}{(4\pi)^{N-n}} \int d^{2N-2n} e_{I_N \setminus C_n} \Omega(\{\vec{e}\}), \qquad (5)$$

i.e., by fixing the spin orientation at the sites of cluster C_n, an average must be taken on all spins outside of the cluster, $i \in I_N \setminus C_n$. Restricting ourselves to one-site and two-site

interactions, Eq. (3) reduces to

$$\Omega(\{\vec{e}\}) \simeq \Omega_0 + \sum_i \sum_{L \neq (0,0)} J_i^L Y_L(\vec{e}_i)$$
$$+ \frac{1}{2} \sum_{i \neq j} \sum_{L \neq (0,0)} \sum_{L' \neq (0,0)} J_{ij}^{LL'} Y_L(\vec{e}_i) Y_{L'}(\vec{e}_j), \quad (6)$$

with

$$\Omega_0 = \langle \Omega \rangle, \qquad (7)$$

$$J_i^L = \int d^2 e_i \langle \Omega \rangle_{\vec{e}_i} Y_L(\vec{e}_i), \qquad (8)$$

and

$$J_{ij}^{LL'} = \int d^2 e_i \int d^2 e_j \langle \Omega \rangle_{\vec{e}_i \vec{e}_j} Y_L(\vec{e}_i) Y_{L'}(\vec{e}_j). \qquad (9)$$

The spin Hamiltonian, Eq. (1) can easily be related to Eq. (6) through the relationships

$$\vec{e}_i \mathbf{K}_i \vec{e}_i = \sum_{m=-2}^{2} J_i^{(2,m)} Y_{2,m}(\vec{e}_i) + \text{const.} \qquad (10)$$

and

$$\vec{e}_i \mathbf{J}_{ij} \vec{e}_j = \sum_{m,m'=-1}^{1} J_{ij}^{(1,m)(1,m')} Y_{1,m}(\vec{e}_i) Y_{1,m'}(\vec{e}_j). \qquad (11)$$

The evaluation of Eq. (5) obviously poses a heavy numerical task since it involves integration of the first-principles grand potential over $N - n$ spin variables. In particular, for infinite systems such as bulk magnets or magnetic films, it seems extremely demanding to ensure the completion of this task. A suitable method is therefore needed that can evaluate the restricted averages in a feasible manner.

B. Relativistic disordered local moment scheme

The disordered local moment (DLM) scheme[10] is an extension to the conventional SDFT to include transverse spin fluctuations. In the DLM scheme the magnetic excitations are modeled by associating local spin-polarization axes with all lattice sites and the orientations $\{\vec{e}\}$ vary very slowly on the time scale of the electronic motion. These "local moment" degrees of freedom produce local magnetic fields centered at the lattice sites which in turn affect the electronic motions and are self-consistently maintained by them. The theory of DLMs in conjunction with the Korringa-Kohn-Rostoker coherent-potential approximation (KKR-CPA) was proposed 25 years ago by Györffy *et al.*[10] and has recently been generalized by Staunton *et al.*[17–19] to include relativistic effects. Here we give a short summary of the method as applied to the consideration of the paramagnetic state.

For spherically symmetric potentials and exchange fields, the local orientation of the spin magnetization is accounted for by the similarity transformation of the single-site matrix,

$$\underline{t}_i(\vec{e}_i) = \underline{D}(\vec{e}_i) \underline{t}_i(\vec{e}_z) \underline{D}(\vec{e}_i)^+, \qquad (12)$$

where for a given energy (not labeled explicitly) $\underline{t}_i(\vec{e}_z)$ stands for the t matrix with the exchange field pointing along the local z axis and $\underline{D}(\vec{e}_i)$ is a (blockwise) projective representation of the SO(3) transformation that rotates the

z axis onto $\vec{e}_i$. Note that underlining indicates matrices in the (κ, μ) angular-momentum representation. In the spirit of the single-site coherent-potential approximation (CPA) an orientation-independent reference medium is introduced in terms of the effective matrices $\underline{t}_{i,c}$ and the corresponding scattering path operator (SPO) matrix

$$\underline{\underline{\tau}}_c = \left(\underline{\underline{t}}_c^{-1} - \underline{\underline{G}}_0 \right)^{-1}. \tag{13}$$

In the above equation, the double underlines denote matrices in site-angular momentum space; $\underline{\underline{t}}_c$ is diagonal in site indices, while $\underline{\underline{G}}_0$ stands for the matrix of structure constants. The effective matrices are determined by the condition that the excess scattering matrices

$$\underline{X}_i(\vec{e}_i) = \left\{ \left[\underline{t}_{i,c}^{-1} - \underline{t}_i^{-1}(\vec{e}_i) \right]^{-1} - \underline{\tau}_{ii,c} \right\}^{-1} \tag{14}$$

vanish when averaged over all possible orientations with an equal probability in the paramagnetic state

$$\frac{1}{4\pi} \int \underline{X}_i(\vec{e}_i) \, d^2 e_i = \underline{0}. \tag{15}$$

The above condition can also be reformulated in terms of the site-diagonal SPO matrices,

$$\langle \underline{\tau}_{ii}(\{\vec{e}\}) \rangle = \frac{1}{4\pi} \int \langle \underline{\tau}_{ii} \rangle_{\vec{e}_i} d^2 e_i = \underline{\tau}_{ii,c}, \tag{16}$$

where the so-called restricted average of the site-diagonal SPO matrix can be expressed as

$$\langle \vec{\tau}_{ii} \rangle_{\vec{e}_i} = \underline{\tau}_{ii,c} \underline{D}_i(\vec{e}_i), \tag{17}$$

with

$$\begin{aligned} \underline{D}_i(\vec{e}_i) &= \underline{I} + \underline{X}_i(\vec{e}_i) \, \underline{\tau}_{ii,c} \\ &= \left\{ \underline{I} + \left[\underline{t}_i^{-1}(\vec{e}_i) - \underline{t}_{i,c}^{-1} \right] \underline{\tau}_{ii,c} \right\}^{-1}. \end{aligned} \tag{18}$$

As discussed in the previous section, we limit our consideration by neglecting longitudinal spin fluctuations; i.e., we suppose that the LSDA potentials and exchange fields are independent of the orientational state $\{\vec{e}\}$. The magnetic force theorem[20] then implies that the LSDA total energy can be replaced by the single-particle energies (band energy) and the grand potential at zero temperature can be expressed as

$$\begin{aligned} \Omega(\{\vec{e}\}) &= E_{\text{LSDA}}(\{\vec{e}\}) - \varepsilon_F N(\{\vec{e}\}) \\ &\simeq - \int^{\varepsilon_F} d\varepsilon \, N(\varepsilon; \{\vec{e}\}). \end{aligned} \tag{19}$$

Here ε_F is the Fermi energy and $N(\varepsilon; \{\vec{e}\})$ denotes the integrated density of states. Using Lloyd's formula[21] and taking the coherent medium as reference, Eq. (19) can be recast as

$$\begin{aligned} \Omega(\{\vec{e}\}) = \Omega_c &- \frac{1}{\pi} \sum_i \text{Im} \int^{\varepsilon_F} d\varepsilon \, \ln \det \underline{D}_i(\vec{e}_i) \\ &- \frac{1}{\pi} \sum_{k=1}^{\infty} \frac{1}{k} \sum_{i_1 \neq i_2 \neq \dots \neq i_k} \text{Im} \int^{\varepsilon_F} d\varepsilon \text{Tr} \left(\underline{X}_{i_1}(\vec{e}_{i_1}) \, \underline{\tau}_{c,i_1 i_2} \right. \\ &\qquad \times \underline{X}_{i_2}(\vec{e}_{i_2}) \cdots \underline{X}_{i_k}(\vec{e}_{i_k}) \, \underline{\tau}_{c,i_k i_1} \Big), \end{aligned} \tag{20}$$

with

$$\Omega_c = - \int^{\varepsilon_F} d\varepsilon \, N_0(\varepsilon) - \frac{1}{\pi} \text{Im} \int^{\varepsilon_F} d\varepsilon \, \ln \det \underline{\underline{\tau}}_c(\varepsilon), \tag{21}$$

where $N_0(\varepsilon)$ represents the integrated density of states of the free electrons.

Equation (20) is, in principle, valid for reference systems fixed by any set of t matrices, $\underline{t}_{c,i}$. The particular choice of the RDLM effective medium, defined by the condition, Eq. (15), is very useful in finding a suitable approximation for the restricted averages in Eq. (5), and consequently for the spin-cluster interactions in Eq. (4). More specifically, when taking averages we neglect the so-called back-scattering contributions in the third term of the right-hand side of Eq. (20), i.e., those for which any site outside of the chosen cluster, $i_l \in I_N \setminus C_n$ ($l = 1, \dots, k$), occurs at least twice. Under this restriction, which is consistent with the single-site CPA,[22] we obtain for the constant term in Eq. (7),

$$\langle \Omega \rangle = \Omega_c - \frac{1}{\pi} \sum_i \text{Im} \int^{\varepsilon_F} d\varepsilon \, \frac{1}{4\pi} \int d^2 e_i \, \ln \det \underline{D}_i(\vec{e}_i). \tag{22}$$

The one-site restricted average of the grand potential can be expressed as

$$\begin{aligned} \langle \Omega \rangle_{\vec{e}_i} = \Omega_c &- \frac{1}{\pi} \text{Im} \int^{\varepsilon_F} d\varepsilon \, \ln \det \underline{D}_i(\vec{e}_i) \\ &- \frac{1}{\pi} \sum_{j(\neq i)} \text{Im} \int^{\varepsilon_F} d\varepsilon \, \frac{1}{4\pi} \int d^2 e_j \, \ln \det \underline{D}_j(\vec{e}_j), \end{aligned} \tag{23}$$

from which one obtains for the one-site expansion coefficient,

$$J_i^L = -\frac{1}{\pi} \text{Im} \int^{\varepsilon_F} d\varepsilon \int d^2 e_i \, \ln \det \underline{D}_i(\vec{e}_i) \, Y_L(\vec{e}_i). \tag{24}$$

From the two-site ($i \neq j$) restricted averages,

$$\begin{aligned} \langle \Omega \rangle_{\vec{e}_i \vec{e}_j} = \Omega_c &- \frac{1}{\pi} \text{Im} \int^{\varepsilon_F} d\varepsilon [\ln \det \underline{D}_i(\vec{e}_i) + \ln \det \underline{D}_j(\vec{e}_j)] \\ &- \frac{1}{\pi} \text{Im} \int^{\varepsilon_F} d\varepsilon \sum_{l(l \neq i,j)} \frac{1}{4\pi} \int d^2 e_l \, \ln \det \underline{D}_l(\vec{e}_l) \\ &- \frac{1}{\pi} \sum_{k=1}^{\infty} \frac{1}{k} \text{Im} \int^{\varepsilon_F} d\varepsilon \, \text{Tr}[(\underline{X}_i(\vec{e}_i) \underline{\tau}_{c,ij} \underline{X}_j(\vec{e}_j) \underline{\tau}_{c,ji})^k], \end{aligned} \tag{25}$$

and using Eq. (9) the following closed expression for the two-spin interactions can be deduced:

$$\begin{aligned} J_{ij}^{LL'} = &-\frac{1}{\pi} \text{Im} \int^{\varepsilon_F} d\varepsilon \iint d^2 e_i \, d^2 e_j \, Y_L(\vec{e}_i) Y_{L'}(\vec{e}) \\ &\times \text{Tr} \ln(\underline{I} - \underline{X}_i(\vec{e}_i) \underline{\tau}_{c,ij} \underline{X}_j(\vec{e}_j) \underline{\tau}_{c,ji}). \end{aligned} \tag{26}$$

In the Appendix we derive the nonrelativistic limit of the above expression.

It is also straightforward to show that a general multispin interaction, as defined in Eq. (4), is given within the RDLM scheme as

$$
J_{C_n}^{L_{i_1}, \ldots, L_{i_n}} = -\frac{1}{\pi} \mathrm{Im} \int^{\varepsilon_F} d\varepsilon \sum_{k \geqslant n} \frac{1}{k} \sum_{i_1 \neq i_2 \neq \cdots \neq i_k}
$$
$$
\times \int d^2 e_{i_1} \ldots \int d^2 e_{i_n} \prod_{l=1}^{n} Y_{L_{i_l}}(\vec{e}_{i_l})
$$
$$
\times \mathrm{Tr}\big(\underline{X}_{i_1}(\vec{e}_{i_1}) \underline{\tau}_{c,i_1 i_2} \underline{X}_{i_2}(\vec{e}_{i_2}) \cdots \underline{X}_{i_k}(\vec{e}_{i_k}) \underline{\tau}_{c,i_k i_1}\big),
$$
$$
(27)
$$

where each term on the right-hand side must contain all the sites in cluster C_n.

III. APPLICATION TO THE IrMn$_3$/Co(111) INTERFACE

A. Computational details

We performed self-consistent calculations for the ordered bulk $L1_2$ IrMn$_3$ alloy, for fcc bulk Co, and for the IrMn$_3$/Co(111) interface in terms of the screened Korringa-Kohn-Rostoker (SKKR) method.[23,24] Because the magnetic structure of the IrMn$_3$/Co(111) interface was not known *a priori*, we employed in these calculations the scalar-relativistic DLM approach that is representative of the para-magnetic state of the system. Here we solved the CPA condition, Eq. (A12), with a relative accuracy of 10^{-5} for the effective matrices. The local spin-density approximation as parametrized by Vosko *et al.*[25] was applied; the effective potentials and fields were treated within the atomic sphere approximation with an angular momentum cutoff of $\ell_{\max} = 2$. The energy integrations were performed by sampling 12 points on a semicircular path in the upper complex semiplane and 84 points were selected in the two-dimensional (2D) Brillouin zone, i.e., in one-fourth of the fcc(111) surface Brillouin zone, for the necessary k integrations. In all cases we used a parent fcc lattice structure with the lattice constant of $L1_2$ IrMn$_3$, $a = 3.785$ Å,[26,27] with no attempt at geometric relaxation.

To ensure that both the IrMn$_3$ and Co components shared the same two-dimensional translational periodicity, which is necessary within the layered SKKR method for an interface, the calculations for Co were carried out with four atoms per cubic unit cell according to the fcc lattice structure. The interface calculations were performed for a symmetric system consisting of two six-monolayer (ML) -thick IrMn$_3$ layers sandwiching a 12 ML Co layer from both sides. Considering four atoms in a unit cell for each layer (three Mn atoms and one Ir atom in each IrMn$_3$ layer and four Co atoms in each Co layer), the total 2D unit cell of the interface system contained 96 atoms. In addition, to ensure smooth boundary conditions, the entire system was sandwiched between two perfect semi-infinite bulk IrMn$_3$ systems as required by the SKKR method.[23,28]

In order to evaluate the integrals over the orientations in Eqs. (24) and (26) we used the efficient Lebedev-Laikov scheme.[29] The energy integration in Eq. (24) was performed by introducing a damping through the Fermi function with $T = 50$ K. The corresponding integral can then be transformed into a sum over the fermionic Matsubara poles and the
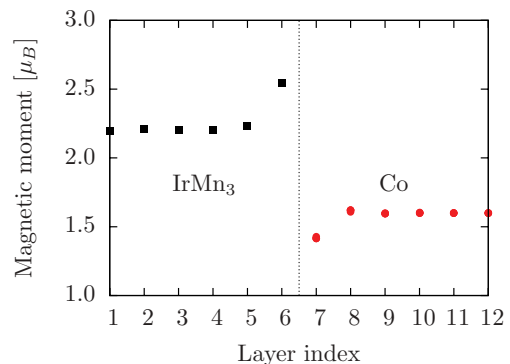

FIG. 1. (Color online) Calculated magnetic moments of Mn and Co atoms for the IrMn$_3$/Co(111) interface. The IrMn$_3$ and Co sides of the interface, marked by the vertical dotted line, correspond to layers labeled by 1–6 and 7–12, respectively.

real part instead of the imaginary part of the logarithm of complex numbers has to be considered, thereby avoiding the well-known phase problem associated with Lloyd's formula.[30] In Eq. (26) this contour integration can safely be used, since the expression $\mathrm{Tr}\ln(\underline{I} - \underline{A})$ in the integrand can be expanded into a rapidly converging power series.

B. Magnetic moments in the DLM state

The self-consistent field calculations resulted in a local magnetic moment of $2.20\mu_B$ for the Mn atoms in $L1_2$ IrMn$_3$. This value is about 15% less than the value we obtained for the spin moment in a relativistic calculation for the ordered triangular ($T1$) state.[9] Such a softening of the magnetic moments is expected in the paramagnetic DLM state due to the vanishing Weiss field acting on the spins. This reduction of the local moment is not necessarily accompanied by a softening of the exchange coupling, however, as is demonstrated below. The calculated local magnetic moment of the fcc bulk Co in the DLM state is $1.62\mu_B$, in agreement with the experimentally and theoretically obtained values for ferromagnetic bulk Co.

In Fig. 1 the magnetic moments for the IrMn$_3$/Co(111) interface system are shown as calculated in the DLM state. Note that only one-half of the symmetric system is shown. Clearly, only moments in close vicinity of the interface are substantially different from their bulk values: the Mn moments increase to $2.54\mu_B$ and the Co moments reduce to $1.42\mu_B$.

C. Isotropic exchange interactions

Recently, we investigated the magnetic ground states of the ordered IrMn$_3$ alloy.[9] In agreement with experiment[26] and other theoretical work,[27] we found that the ground-state spin structure of the Mn sublattices is a frustrated 120° Néel-type state in the (111) planes of the fcc lattice, called the $T1$ state. This frustration is the consequence of the strong antiferromagnetic exchange coupling between the Mn atoms. In Fig. 2 we compare the isotropic exchange interactions, $J_{ij} = (1/3)\mathrm{Tr}\,\mathbf{J}_{ij}$, obtained from the SCE-RDLM scheme with those from the RTM.[11] Clearly the two sets of parameters (circles and squares) are in very good quantitative agreement. This indicates that the softening of the magnetic moments in the DLM state does not imply a softening of the exchange
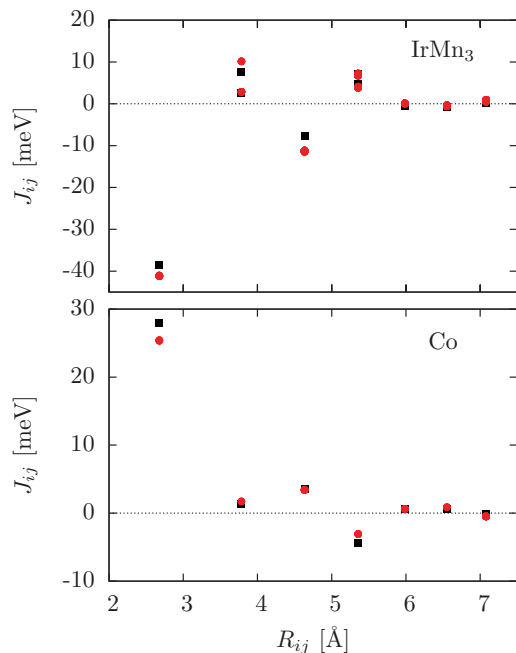
FIG. 2. (Color online) Calculated isotropic exchange interactions J_{ij} for bulk $L1_2$ IrMn$_3$ (upper panel) and fcc bulk Co (lower panel). Squares and circles refer to the J_{ij}'s obtained from the DLM states by using the SCE-RDLM method and by using the RTM,[11] using the ordered ground state (the $T1$ state for IrMn$_3$ and the ferromagnetic state for Co), respectively. The interactions are displayed as a function of the distance, R_{ij}.

couplings with respect to the ordered state. In contrast to IrMn$_3$, the exchange interactions of bulk Co are primarily of ferromagnetic nature. A very good agreement between the SCE-RDLM and the RTM can also be seen in this case. Importantly, both systems are characterized by short-range interactions: the J_{ij}'s practically vanish beyond the fourth neighbor shell.

For the 6 ML IrMn$_3$/12 ML Co/6 ML IrMn$_3$ interface system we considered all the pairs of magnetic atoms separated by a distance less than 10.68 Å. This implied the calculation of a total number of more than 13 000 tensorial interactions. Inspection of the calculated isotropic exchange interactions reveals that the Mn-Mn and Co-Co interactions are spread around their corresponding bulk values due to symmetry breaking at the interface: the nearest-neighbor (NN) Mn-Mn interactions are somewhat increased, while most of the NN Co-Co interactions are decreased. This decrease is of up to 20% near the interface. This feature clearly correlates with the change of the local magnetic moments caused by the presence of the interface depicted in Fig. 1. The Mn-Co interactions across the interface are quite small in magnitude (<10 meV) and mostly antiferromagnetic: $J_{ij} = -6.15$ meV for nearest neighbors, while $J_{ij} = -4.86$ and -8.40 meV for next-nearest neighbors.

In order to visualize the isotropic exchange interactions for the interface system, we defined the following effective interaction parameters:

$$J_{pi} = \sum_{q,j} J_{pi,qj} \, \vec{e}_{pi} \cdot \vec{e}_{qj}, \qquad (28)$$
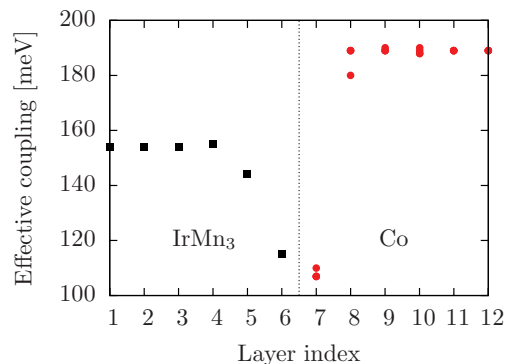

FIG. 3. (Color online) Calculated effective exchange interactions for the IrMn$_3$/Co interface as defined in Eq. (28). The labeling of layers is identical to that in Fig. 1.

where p and q denote layers, while i and j stand for sites within the corresponding layers. For this calculation we choose a magnetic state $\{\vec{e}_{pi}\}$ corresponding to the $T1$ structure for the IrMn$_3$ side and to an FM state perpendicular to the interface within the Co layers. This configuration was chosen because of the antiferromagnetic nature of the interface coupling combined with the large Mn anisotropy, which constrains the $T1$ structure within the interface plane. Clearly, by translational and rotational symmetry of this spin structure, J_{pi} turned out to be the same for all the Mn sites in a given layer p of the IrMn$_3$ region, while in each layer of the Co region, in principle, two different values for J_{pi} may be obtained. In particular, for the Co layer adjacent to IrMn$_3$, these two different values are associated with Co sites having two and three NN Mn atoms.

Figure 3 clearly shows that the effective exchange interactions quickly approach their bulk value with distance from the interface. This follows from the fact that only interactions between atoms in close proximity to the interface deviate from their counterparts in the bulk; those more than two atomic planes away from the interface are practically bulklike. Such behavior is to be expected because of the very narrow range of exchange interactions in the bulk systems. Since for the chosen magnetic states the magnetic orientations of the Mn and Co atoms are perpendicular to each other, the otherwise weak Mn-Co interactions are excluded from the sum in Eq. (28) and the effective interactions are significantly decreased near the interface. The different values of J_{pi} for the nonequivalent Co sites near to the interface can also be seen in the figure.

D. Magnetic anisotropies

The most remarkable observation of our previous study[9] was the surprisingly strong, second-order magnetic anisotropies of IrMn$_3$ resulting from the fact that the cubic symmetry is locally broken for each of the three Mn sublattices. Rotating the $T1$ state around the axis normal to the (111) plane, the energy of the system can be described as $E(\varphi) = E_0 + K_{\text{eff}} \sin^2 \varphi$. By calculating $E(\varphi)$ in the $T1$ spin state, a value of $K_{\text{eff}} = 10.4$ meV was deduced.[9] We repeated this calculation by using the self-consistent field potentials from the DLM state and obtained a value of $K_{\text{eff}} = 7.67$ meV. Although this value is about 30% less than the one we obtained in our previous calculation using the $T1$ ground state, it is

still consistent with the observation of a very large magnetic anisotropy.

The SCE-RDLM scheme provides a unique opportunity to calculate contributions of the MAE related to the one-site and the two-site exchange anisotropy terms, which is an important issue for spin-model simulations because it affects the scaling of the anisotropy with magnetization. First we note that, by symmetry, in the frame of reference with the z axis along the (111) direction, the one-site anisotropy matrices of the three Mn sublattices in the $L1_2$ phase can be expressed as

$$\mathbf{K}_1^{(111)} = K \begin{pmatrix} 0 & 0 & 0 \\ 0 & \frac{2}{3} & -\frac{\sqrt{2}}{3} \\ 0 & -\frac{\sqrt{2}}{3} & \frac{1}{3} \end{pmatrix},$$ (29)

$$\mathbf{K}_2^{(111)} = K \begin{pmatrix} \frac{1}{2} & -\frac{\sqrt{3}}{6} & -\frac{\sqrt{6}}{6} \\ -\frac{\sqrt{3}}{6} & \frac{1}{6} & \frac{\sqrt{2}}{6} \\ -\frac{\sqrt{6}}{6} & \frac{\sqrt{2}}{6} & \frac{1}{3} \end{pmatrix},$$ (30)

$$\mathbf{K}_3^{(111)} = K \begin{pmatrix} \frac{1}{2} & \frac{\sqrt{3}}{6} & \frac{\sqrt{6}}{6} \\ \frac{\sqrt{3}}{6} & \frac{1}{6} & \frac{\sqrt{2}}{6} \\ \frac{\sqrt{6}}{6} & \frac{\sqrt{2}}{6} & \frac{1}{3} \end{pmatrix}.$$ (31)

Our calculations based on Eqs. (10) and (24) confirmed with high accuracy these nontrivial forms of the one-site anisotropy matrices, with a value of $K = 0.82$ meV. Note that the total one-site contribution to $K_{\rm eff}$ is $2K$.[9] In addition, from the tensorial exchange interactions, Eqs. (9) and (11), we calculated a two-site anisotropy contribution of 6.73 meV to the MAE. Thus, the spin Hamiltonian derived from the SCE-RDLM approach yielded $K_{\rm eff} = 8.37$ meV, in good agreement with $K_{\rm eff} = 7.67$ meV we calculated directly from the band energy. The difference between the two values should be related to the fact that the direct calculation of the MAE is not restricted to second-order interactions as is the case for the spin Hamiltonian. Due to cubic symmetry, for fcc bulk Co we calculated negligible MAE, $|K_{\rm eff}| < 1$ μeV.

Next we investigated the magnetic anisotropy of the spin structure described in the context of Eq. (28) and Fig. 3 for the interface system. Of particular interest is the variation of the energy, Eq. (1), during a magnetization reversal process. For transparency, we considered the reversal of the Co moments from z to $-z$ by keeping the relative orientations of any two moments in the system fixed. Theoretically, this is equivalent to rotating all the spins simultaneously around an axis in the (111) plane by an angle of $0 \leqslant \varphi \leqslant \pi$. Clearly from Eq. (1) the energy $E(\varphi)$ can be recast into layerwise contributions $E_p(\varphi)$ such that

$$E(\varphi) = N \sum_p E_p(\varphi),$$ (32)

where N is the number of cells in a layer and $E_p(\varphi)$ comprises the contributions of three Mn atoms and four Co atoms in the IrMn$_3$ and Co parts of the interface system. Moreover, $E_p(\varphi)$ can be decomposed into contributions arising from the one- and two-site terms of Eq. (1).

Note that in these calculations only the symmetric part of the tensorial exchange matrices, $\mathbf{J}_{ij}^s = \frac{1}{2}(\mathbf{J}_{ij} + \mathbf{J}_{ij}^T)$, was
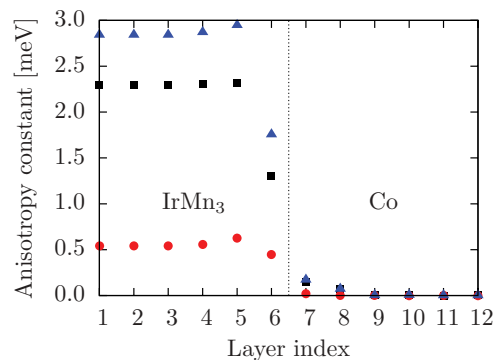

FIG. 4. (Color online) Calculated effective anisotropy parameters (triangles) $K_{\rm eff}^p$, see Eq. (32), for the IrMn$_3$/Co interface. Also shown are the corresponding one-site ($K_{\rm eff}^{p,{\rm os}}$, circles) and two-site ($K_{\rm eff}^{p,{\rm ts}}$, squares) contributions.

considered. Our numerical results confirmed that the following forms of $E_p(\varphi)$, which describe the bulk anisotropy energies,[9] give a good description for the layered system as well:

$$E_p(\varphi) = E_p(0) + \frac{K_{\rm eff}^p}{8}[2 + \sin^2 \varphi - 2\cos\varphi$$
$$- 2\sqrt{2}\sin\varphi(1 - \cos\varphi)]$$ (33)

for the IrMn$_3$ layers and

$$E_p(\varphi) = E_p(0) + K_{\rm eff}^p \sin^2 \varphi$$ (34)

for the Co layers.

In Fig. 4 the layer-resolved effective anisotropy parameters $K_{\rm eff}^p$ are normalized to one Mn (layers 1–6) and Co (layers 7–12) atom, together with their one-site and two-site contributions. Reassuringly, when departing from the interface these functions show a stable convergence to the corresponding bulk values $K_{\rm eff}^p = 2.79$ meV, $K_{\rm eff}^{p,{\rm os}} = 0.54$ meV, and $K_{\rm eff}^{p,{\rm ts}} = 2.28$ meV for IrMn$_3$, and $K_{\rm eff}^p \simeq K_{\rm eff}^{p,{\rm os}} \simeq K_{\rm eff}^{p,{\rm ts}} \simeq 0$ for Co. In the vicinity of the interface, $K_{\rm eff}^{p,{\rm os}}$ of Mn shows moderate oscillations and $K_{\rm eff}^{p,{\rm os}}$ of Co is still below the 0.01–0.02 meV range. The two-site anisotropy contribution at the IrMn$_3$ layer nearest to the interface drops, however, to half of the bulk value. The absence of Mn-Mn interactions at the interface reduces the nearest-neighbor coordination of the interface Mn spins from 8 to 6; the decrease observed indicates therefore that some softening of the intrinsic Mn anisotropy is found at the interface. Breaking of the cubic bulk symmetry, i.e., missing the Co planes from one side, also results in an increase to about 0.22 meV of the Co $K_{\rm eff}^{p,{\rm ts}}$ at the interface.

E. Dzyaloshinskii-Moriya interactions

The antisymmetric components of the exchange interactions, $\mathbf{J}_{ij}^a = \frac{1}{2}(\mathbf{J}_{ij} - \mathbf{J}_{ij}^T)$, correspond to the well-known Dzyaloshinskii-Moriya (DM) interaction.[31,32] The DM interaction favors perpendicular alignment of moments and for a given pair of spins, the antisymmetric component of the exchange interaction may be conveniently represented by the DM vector $\vec{D}_{ij}$,

$$\vec{e}_i \mathbf{J}_{ij}^a \vec{e}_j = \vec{D}_{ij} \cdot (\vec{e}_i \times \vec{e}_j).$$ (35)

In the $L1_2$ structure, the absence of inversion symmetry at the Mn lattice points gives rise to a DM interaction with a magnitude of 1.24 meV between nearest neighbors, with $\vec{D}_{ij}$ aligned along the $(1\bar{2}\bar{2})$ directions. Following the trend of the isotropic exchange interactions, the magnitudes of the DM interactions diminish very rapidly with distance; the third and fifth NN interactions in the bulk are 0.58 and 0.13 meV, respectively. Clearly enough, in a noncollinear ground state of a bulk system, the asymmetric contribution to the exchange interaction might be nonzero only for different sublattices. However, due to symmetry, the intersublattice DM interactions also give rise to no overall magnetic anisotropy energy in bulk $L1_2$ IrMn$_3$.

Calculations reveal that the symmetry breaking at the IrMn$_3$/Co interface gives rise to additional asymmetry in the exchange interactions at the interface. Although restricted to the atomic planes in the immediate vicinity of the interface, these interactions cause an anisotropy contribution for the reversal process discussed in the context of Fig. 4 that arises purely due to the presence of the interface and shows an angular dependence that is unidirectional,

$$E_p^{\text{DM}}(\varphi) = E_p(0) + K_p^{\text{DM}} \cos \varphi. \qquad (36)$$

K_p^{DM} is plotted for the interface structure in Fig. 5. The reduced coordination of the interface Mn spins gives rise to a large anisotropic DM contribution to the system energy. Specifically, at the interface the antisymmetric exchange components give rise to an additional energy difference between the $T1$ and $T2$ Mn spin configurations, related to different chirality.[9]

Concerning the Co layers, a value of -0.19 meV for the DM anisotropy energies (shown in Fig. 5) denotes a unidirectional anisotropy favoring alignment of the Co spins perpendicular to, or away from, the interface plane. This anisotropy arises in the antisymmetric components of the interface Co-Mn interactions. The DM vectors for the interface exchange interactions are depicted as solid arrows in Fig. 6, where $\vec{D}_{ij}$ is shown when i indexes a Co site and j a Mn site.

The interface DM vectors are found to lie almost entirely in the interface plane which favors a perpendicular spin alignment of the Co relative to the interface. Which of the two perpendicular directions is favored depends upon the sense of the DM vectors and the Mn spin configuration: for the
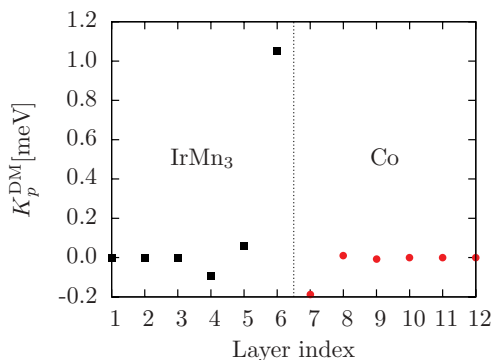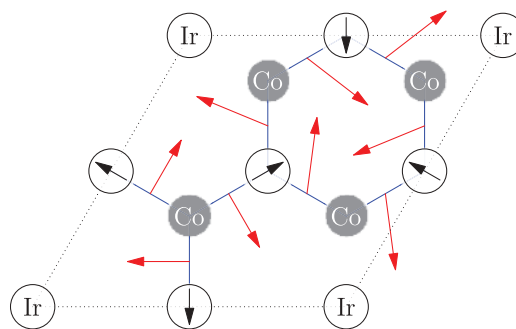

FIG. 6. (Color online) The arrows show the (111) in-plane projections of the DM vectors $\vec{D}_{ij}$ for nearest-neighbor interface Co-Mn interactions. The $T1$ configuration of the Mn spins is indicated by arrows within circles at the Mn positions. Note that the planes of the Co atoms are above the IrMn$_3$ layer.

Mn configuration shown in Fig. 6, Co alignment away from the IrMn$_3$ layer is preferred. Simultaneous inversion of the spins on all three Mn sublattices, which does not affect the chirality of the Mn spin structure, produces a configuration that is energetically equivalent in the bulk, but which causes the preferred orientation of the Co layers at an interface to be reversed. Note, however, that such a change in the Mn spin configuration cannot be obtained by any single global rotation.

IV. CONCLUSIONS

We have introduced a computational scheme to calculate magnetic anisotropy parameters and tensorial exchange interactions based on a spin-cluster expansion and the relativistic disordered local moment picture of itinerant magnets. The method relies on the high-temperature paramagnetic phase, thus, it is uniquely applicable to any system with arbitrary magnetic ground state. In particular, it is highly efficient in cases when the complex magnetic structure of the system is not known *a priori* from first-principles total-energy calculations, such as for heterogeneous interfaces and nanoparticles. Moreover, the SCE-RDLM method can be used to calculate higher-order multispin interactions. The main limitation of the method is that longitudinal spin fluctuations are neglected: in the case of large induced moments, further extension of the theory is needed.[33] Moreover, the magnetic short-range order suppressed in a DLM description of the paramagnetic phase can influence (increase) the nearest-neighbor interactions.[34] However, as indicated by Fig. 2, this effect does not seem to be of crucial importance for the IrMn$_3$/Co interface system.

We applied the method to calculate magnetic anisotropies and spin interactions at an IrMn$_3$/Co(111) interface. Our main observation is that the corresponding bulk properties are influenced in the immediate vicinity of the interface only. The exchange interactions between the Mn and Co atoms are weak leaving the corresponding bulk magnetic structures fairly unaffected even at the interface. Symmetry breaking at the interface gives rise, however, to large anisotropy effects. Most prominently, the appearance of sizable Dzyaloshinskii-Moriya interactions at the interface results in a perpendicular coupling of the Co and Mn spins and in a unidirectional exchange anisotropy that might substantially influence the exchange bias in such systems.[35–37] By using the spin-model parameters

FIG. 5. (Color online) Calculated layerwise anisotropy constants due to DM interactions, K_p^{DM}; see Eq. (36) for the IrMn$_3$/Co interface.

derived in this work, we are going to present a detailed study to explore the spin dynamics and the exchange bias properties of the IrMn$_3$/Co(111) interface.

APPENDIX: NONRELATIVISTIC LIMIT OF THE TENSORIAL EXCHANGE INTERACTIONS

In order to derive a nonrelativistic limit of the SCE-RDLM formalism for the two-site exchange interactions we first expand the logarithm to first order in Eq. (26),

$$J_{ij}^{LL'} = \frac{1}{\pi} \text{Im} \int^{\varepsilon_F} d\varepsilon \, \text{Tr} \, (\underline{X}_{i,L} \, \underline{\tau}_{c,ij} \, \underline{X}_{j,L'} \, \underline{\tau}_{c,ji}), \quad \text{(A1)}$$

with

$$\underline{X}_{i,L} = \int d^2 e_i \, \underline{X}_i(\vec{e}_i) Y_L^*(\vec{e}_i), \quad \text{(A2)}$$

where, for convenience, but in this section only, we use complex spherical harmonics. In the nonrelativistic case the transformation(12) applies in spin space only,

$$t_i^{ss'}(\vec{e}_i) = \underline{t}_{i,0} \delta_{ss'} + \Delta \underline{t}_i \, \vec{\sigma}_{ss'} \, \vec{e}_i \, , \quad \text{(A3)}$$

where $\underline{t}_{i,0}$ and $\Delta \underline{t}_i$ are now matrices in nonrelativistic angular momentum (ℓ,m) space, $\vec{\sigma}$ are the Pauli matrices, and $s = \uparrow,\downarrow$ denotes the spin index. Clearly, the usual spin-up and spin-down components of the t matrices are

$$\underline{t}_i^{\uparrow} = \underline{t}_{i,0} + \Delta \underline{t}_i, \quad \text{(A4)}$$

$$\underline{t}_i^{\downarrow} = \underline{t}_{i,0} - \Delta \underline{t}_i, \quad \text{(A5)}$$

while for the paramagnetic case the effective t matrices and SPO matrices become diagonal in spin space,

$$\underline{t}_{i,c}^{ss'} = \underline{t}_{i,c} \delta_{ss'}, \quad \text{(A6)}$$

$$\underline{\tau}_{ij,c}^{ss'} = \underline{\tau}_{ij,c} \delta_{ss'}. \quad \text{(A7)}$$

Since also the excess scattering matrices take the form of Eqs. (A3)–(A5),

$$\underline{X}_i^{ss'}(\vec{e}_i) = \underline{X}_{i,0} \delta_{ss'} + \Delta \underline{X}_i \, \overrightarrow{\sigma}_{ss'} \vec{e}_i, \quad \text{(A8)}$$

with

$$\underline{X}_i^{\uparrow} = \underline{X}_{i0} + \Delta \underline{X}_i, \quad \text{(A9)}$$

$$\underline{X}_i^{\downarrow} = \underline{X}_{i0} - \Delta \underline{X}_i, \quad \text{(A10)}$$

and

$$\underline{X}_i^s = \left\{ \left[\underline{t}_{i,c}^{-1} - \left(\underline{t}_i^s \right)^{-1} \right]^{-1} - \underline{\tau}_{ii,c} \right\}^{-1} (s = \uparrow,\downarrow), \quad \text{(A11)}$$

the CPA condition(15) can be rewritten as

$$\frac{1}{2}(\underline{X}_i^{\uparrow} + \underline{X}_i^{\downarrow}) = 0. \quad \text{(A12)}$$

The integration over angular variables can be explicitly performed in Eq. (A2),

$$\underline{X}_{i,L} = \Delta \underline{X}_i \, \vec{\sigma} \int d^2 e_i Y_L^*(\vec{e}_i) \vec{e}_i \left(\frac{4\pi}{3} \right)^{1/2}$$
$$\times \Delta \underline{X}_i (2\delta_{L,(1,-1)} \sigma_+ - 2\delta_{L,(1,1)} \sigma_- + \delta_{L,(1,0)} \sigma_z), \quad \text{(A13)}$$

with $\sigma_\pm = \sigma_x \pm i\sigma_y$. The trace in Eq. (A1) can then be recast into a trace in angular momentum space, Tr$_L$, and a trace in spin space, Tr$_s$,

$$\text{Tr} \, (\underline{X}_{i,L} \, \underline{\tau}_{c,ij} \, \underline{X}_{j,L'} \, \underline{\tau}_{c,ji})$$
$$= \frac{4\pi}{3} \text{Tr}_L(\Delta \underline{X}_i \, \underline{\tau}_{c,ij} \, \Delta \underline{X}_j \, \underline{\tau}_{c,ji})$$
$$\times \text{Tr}_s[(2\delta_{L,(1,-1)} \sigma_+ - 2\delta_{L,(1,1)} \sigma_- + \delta_{L,(1,0)} \sigma_0)$$
$$\times (2\delta_{L',(1,-1)} \sigma_+ - 2\delta_{L',(1,1)} \sigma_- + \delta_{L',(1,0)} \sigma_0)]. \quad \text{(A14)}$$

By using the algebra of the Pauli matrices, the trace in spin space can easily be performed and the two-site terms in the spin Hamiltonian will be transformed into a pure isotropic Heisenberg interaction,

$$\sum_{LL'} J_{ij}^{LL'} Y_L(\vec{e}_i) Y_{L'}^*(\vec{e}_j) = J_{ij} \vec{e}_i \vec{e}_j, \quad \text{(A15)}$$

with

$$J_{ij} = -\frac{2}{\pi} \text{Im} \int^{\varepsilon_F} d\varepsilon \, \text{Tr}_L(\Delta \underline{X}_i \, \underline{\tau}_{c,ij} \, \Delta \underline{X}_j \, \underline{\tau}_{c,ji}) \quad \text{(A16)}$$

$$= -\frac{1}{2\pi} \text{Im} \int^{\varepsilon_F} d\varepsilon \, \text{Tr}_L[(\underline{X}_i^{\uparrow} - \underline{X}_i^{\downarrow})\underline{\tau}_{c,ij}(\underline{X}_j^{\uparrow} - \underline{X}_j^{\downarrow})\underline{\tau}_{c,ji}]. \quad \text{(A17)}$$

This formula is widely used in nonrelativistic calculations of the exchange interactions.[38]

---

*szunyogh@phy.bme.hu

[1]W. H. Meiklejohn and C. P. Bean, Phys. Rev. **102**, 1413 (1956); **105**, 904 (1957).

[2]J. Nogués and I. K. Schuller, J. Magn. Magn. Mater. **192**, 203 (1999).

[3]A. P. Malozemoff, Phys. Rev. B **35**, 3679 (1987).

[4]P. Miltényi, M. Gierlings, J. Keller, B. Beschoten, G. Güntherodt, U. Nowak, and K. D. Usadel, Phys. Rev. Lett. **84**, 4224 (2000).

[5]U. Nowak, A. Misra, and K. D. Usadel, J. Magn. Magn. Mater. **240**, 243 (2002).

[6]G. Scholten, K. D. Usadel, and U. Nowak, Phys. Rev. B **71**, 064413 (2005).

[7]K. O'Grady, L. E. Fernandez-Outon, and G. Vallejo-Fernandez, J. Magn. Magn. Mater. **322**, 883 (2010).

[8]R. Y. Umetsu, A. Sakuma, and K. Fukamichi, Appl. Phys. Lett. **89**, 052504 (2006).

[9]L. Szunyogh, B. Lazarovits, L. Udvardi, J. Jackson, and U. Nowak, Phys. Rev. B **79**, 020403(R) (2009).

[10]B. L. Györffy, A. J. Pindor, J. B. Staunton, G. M. Stocks, and H. Winter, J. Phys. F: Met. Phys. **15**, 1337 (1985).

[11] L. Udvardi, L. Szunyogh, K. Palotás, and P. Weinberger, Phys. Rev. B **68**, 104436 (2003).

[12] H. Ebert and S. Mankovsky, Phys. Rev. B **79**, 045209 (2009).

[13] A. Antal, B. Lazarovits, L. Udvardi, L. Szunyogh, B. Újfalussy, and P. Weinberger, Phys. Rev. B **77**, 174429 (2008).

[14] Ph. Kurz, G. Bihlmayer, K. Hirai, and S. Blügel, Phys. Rev. Lett. **86**, 1106 (2001).

[15] R. Drautz and M. Fähnle, Phys. Rev. B **69**, 104404 (2004).

[16] R. Drautz and M. Fähnle, Phys. Rev. B **72**, 212405 (2005).

[17] J. B. Staunton, S. Ostanin, S. S. A. Razee, B. L. Györffy, L. Szunyogh, B. Ginatempo, and E. Bruno, Phys. Rev. Lett. **93**, 257204 (2004).

[18] J. B. Staunton, L. Szunyogh, A. Buruzs, B. L. Györffy, S. Ostanin, and L. Udvardi, Phys. Rev. B **74**, 144411 (2006).

[19] A. Buruzs, P. Weinberger, L. Szunyogh, L. Udvardi, P. I. Chleboun, A. M. Fischer, and J. B. Staunton, Phys. Rev. B **76**, 064417 (2007).

[20] H. J. F. Jansen, Phys. Rev. B **59**, 4699 (1999).

[21] P. Lloyd, Proc. Phys. Soc. London **90**, 207 (1967).

[22] W. H. Butler, Phys. Rev. B **31**, 3260 (1985).

[23] L. Szunyogh, B. Újfalussy, P. Weinberger, and J. Kollár, Phys. Rev. B **49**, 2721 (1994).

[24] R. Zeller, P. H. Dederichs, B. Újfalussy, L. Szunyogh, and P. Weinberger, Phys. Rev. B **52**, 8807 (1995).

[25] S. H. Vosko, L. Wilk, and M. Nusair, Can. J. Phys. **58**, 1200 (1980).

[26] I. Tomeno, H. N. Fuke, H. Iwasaki, M. Sahashi, and Y. Tsunoda, J. Appl. Phys. **86**, 3853 (1999).

[27] A. Sakuma, K. Fukamichi, K. Sasao, and R. Y. Umetsu, Phys. Rev. B **67**, 024420 (2003).

[28] J. Zabloudil, R. Hammerling, L. Szunyogh, and P. Weinberger, *Electron Scattering in Solid Matter*, Springer Series in Solid-State Sciences Vol. 147 (Springer, Heidelberg, 2005).

[29] V. I. Lebedev and D. N. Laikov, Dokl. Math. **59**, 477 (1999).

[30] R. Zeller, J. Phys.: Condens. Matter **17**, 5367 (2005).

[31] I. Dzyaloshinskii, J. Phys. Chem. Solids **4**, 241 (1958).

[32] T. Moriya, Phys. Rev. **120**, 91 (1960).

[33] O. N. Mryasov, Phase Transitions **78**, 197 (2005).

[34] V. Antropov, Phys. Rev. B **72**, 140406(R) (2005).

[35] T. C. Schultess and W. H. Butler, Phys. Rev. Lett. **81**, 4516 (1998).

[36] I. N. Krivorotov, C. Leighton, J. Nogués, Ivan K. Schuller, and E. D. Dahlberg, Phys. Rev. B **68**, 054430 (2003).

[37] S. Dong, K. Yamauchi, S. Yunoki, R. Yu, S. Liang, A. Moreo, J.-M. Liu, S. Picozzi, and E. Dagotto, Phys. Rev. Lett. **103**, 127201 (2009).

[38] M. Ondráček, O. Bengone, J. Kudrnovský, V. Drchal, F. Máca, and I. Turek, Phys. Rev. B **81**, 064410 (2010).